

# On the gluon content of the $\pi$ and $\rho^0$ mesons

---

Rafel Escribano

Grup de Física Teòrica and IFAE, Universitat Autònoma de Barcelona, E-08193  
 Bellaterra (Barcelona), Spain  
 E-mail: Rafel.Escribano@ifae.es

Jordi Nadal

Institut de Física d'Àrees Energètiques, Universitat Autònoma de Barcelona, E-08193  
 Bellaterra (Barcelona), Spain  
 E-mail: jnadal@ifae.es

**Abstract:** A phenomenological analysis of radiative  $V \rightarrow P \gamma$  and  $P \rightarrow V \gamma$  decays is performed with the purpose of determining the gluonic content of the  $\pi$  and  $\rho^0$  wave functions. Our results show that there is no evidence for a gluonium contribution in the  $\pi$ ,  $Z^2_0 = 0.00 \pm 0.07$ , or the  $\rho^0$ ,  $Z^2_0 = 0.04 \pm 0.09$ . In terms of a mixing angle description this corresponds to  $\rho = (41.4 \pm 1.3)$  and  $j_{\text{G}} = (12 \pm 13)$ . In addition, the  $\rho^0$  mixing angle is found to be  $\rho = (41.5 \pm 1.2)$  if we don't allow for a gluonium component.

**Keywords:** pion, empirical

---

## Contents

1. Introduction	1
2. Notation	2
3. A model for $V P \rightarrow M 1$ transitions	3
4. Data fitting	4
5. Comparison with other approaches	8
6. Summary and conclusions	13
A. Euler angles	13

---

## 1. Introduction

Very recently, the KLOE Collaboration has reported a new measurement of the ratio  $R = B(\pi^0 \rightarrow \pi^0) = B(\pi^+ \rightarrow \pi^0)$  [1]. Combining the value of  $R$  with other constraints, they have estimated the gluonium content of the  $\pi^0$  meson as  $Z^2_{\pi^0} = 0.14 \pm 0.04$ , which points to a significant gluonium fraction in the  $\pi^0$  wave function incompatible with zero by more than 3%. This new result contrasts with the former value  $Z^2_{\pi^0} = 0.06^{+0.09}_{-0.06}$ , which was compatible with zero within 1% and consistent with a gluonium fraction below 15% [2]. Both experimental analysis obtain their results using the same set of constraints derived from other measured ratios, namely<sup>1</sup>  $(\pi^0 \pi^0) = (\pi^0 \pi^+ \pi^-)$ ,  $(\pi^0 \pi^+ \pi^-) = (\pi^+ \pi^+ \pi^-)$  and  $(\pi^0 \pi^+ \pi^-) = (\pi^+ \pi^+ \pi^0)$ , as well as  $R$ . The sole difference between the two analyses, apart from the obvious improvement in the precision of the new measurements, is the inclusion in the amplitudes of Ref. [1] of two extra parameters to deal with the overlap of the vector and pseudoscalar meson wave functions produced in the transitions  $V \rightarrow P$  or  $P \rightarrow V$ , a feature first introduced in Ref. [3]. However, the new analysis of Ref. [1] uses the most recent experimental data taken from Ref. [4] in association with the values for the parameters related to the overlap which were obtained in Ref. [3] from a fit to available experimental data at that time. Therefore, a reanalysis of this uncomfortable situation is needed before drawing definite conclusions on the gluon content of the  $\pi^+$  and  $\pi^0$  mesons. The purpose of this work is to perform a phenomenological analysis of radiative  $V \rightarrow P$  and  $P \rightarrow V$  decays, with  $V = \pi, K, \eta$ ; and  $P = \pi^0, K^0, \eta^0$ , aimed at determining

---

<sup>1</sup>The analysis in Ref. [2] did not contain the constraint imposed by  $(\pi^0 \pi^+ \pi^-) = (\pi^+ \pi^+ \pi^0)$ . Nevertheless, the inclusion of this constraint does not change the main results of the analysis, as seen in Ref. [1].

the gluonic content of the  $^0$  and  $^1$  wave functions. Similar analysis were driven in the seminal work by Rosner [5], where the allowed gluonic admixture in the  $^0$  was found to be small,  $\mathcal{Z} \approx 0.4$ , but not necessarily zero. The gluonic content of the  $^0$  could not be established due to the lack of data on  $^1$ . Later on, Kou pointed out that the  $^0$  gluonic component might be as large as 26% [6]. These two works also included in their analysis the constraints provided by  $P^1$  with  $P = 0$ . Here, we will not take into account these decays since they are nicely described in a two mixing angle scheme, as shown in Refs. [7, 8]. A more recent analysis studying the pseudoscalar glueball- $qq$  mixing from  $J=0$   $^1$  VP decays gets  $\mathcal{Z} \approx 0.042$  and  $\mathcal{Z} \approx 0.161$  [9].

In Sec. 2, we briefly introduce the notation. The model for  $V P \rightarrow M 1$  transitions to be used in our analysis is presented in Sec. 3. This model includes the overlap of vector and pseudoscalar wave functions as a main ingredient [3]. As stated above, the use of old values for the overlap parameters in addition to the latest data may be at the origin of the discrepancy concerning the gluon content of the  $^0$  between the two KLOE analyses [1, 2]. Sec. 4 is devoted to the data fitting of the most recent  $V \rightarrow P$  and  $P \rightarrow V$  experimental data with the aim of finding the gluonic admixture in the  $^0$  and  $^1$  wave functions. As a matter of comparison with other approaches, a graphical representation of our main results is shown in Sec. 5. Finally, in Sec. 6 we summarize our work and present the conclusions. A decomposition of the mixing parameters in terms of Euler angles is left for App. A.

## 2. Notation

We will work in a basis consisting of the states  $j_{qi} = \frac{1}{2} j_{uu} + d_{di}$ ,  $j_{si} = j_{ssi}$  and  $j_{gi}$  gluonium. The physical states  $^0$  and  $^1$  are assumed to be linear combinations of these:

$$\begin{aligned} j_i &= X j_{qi} + Y j_{si} + Z j_{gi}; \\ j^0_i &= X^0 j_{qi} + Y^0 j_{si} + Z^0 j_{gi}; \end{aligned} \quad (2.1)$$

with  $X^2 + Y^2 + Z^2 = 1$  and thus  $X^2 + Y^2 = 1$ . A significant gluonic admixture in a state is possible only if  $Z^2 = 1 - X^2 - Y^2 > 0$  [5]. This mixing scheme assumes isospin symmetry, i.e. no mixing with  $^0$ , and neglects other possible admixtures from cc states and/or radial excitations. In absence of gluonium,  $Z = 0$ , the mixing parameterization (2.1) is reduced to the standard pattern in the quark-avour basis

$$\begin{aligned} j_i &= \cos \varphi j_{qi} - \sin \varphi j_{si}; \\ j^0_i &= \sin \varphi j_{qi} + \cos \varphi j_{si}; \end{aligned} \quad (2.2)$$

with  $X = Y = \cos \varphi$ ,  $X^0 = -Y = \sin \varphi$ , and  $X^2 + Y^2 = 1$ . Similarly, for the vector states  $^1$  and the mixing is given by

$$\begin{aligned} j^1_i &= \cos \psi j_{qi} - \sin \psi j_{si}; \\ j^0_i &= \sin \psi j_{qi} + \cos \psi j_{si}; \end{aligned} \quad (2.3)$$

where  $j^1_{qi}$  and  $j^0_{si}$  are the analog non-strange and strange states of  $j_{qi}$  and  $j_{si}$ , respectively.

### 3. A model for VP M 1 transitions

We will work in a conventional quark model context and assume that pseudoscalar and vector mesons are simple quark-antiquark S-wave bound states. All these hadrons are thus extended objects with characteristic spatial extensions fixed by their respective quark-antiquark P or V wave functions. In the pseudoscalar nonet,  $P = \{K^0, \bar{K}^0, \pi^0, \bar{\pi}^0, \eta, \bar{\eta}, \eta', \bar{\eta}', \eta''\}$ , the quark spins are antiparallel and the mixing pattern is given by Eq. (2.1). In the vector case,  $V = \{K^+, \bar{K}^+, \pi^+, \bar{\pi}^+, \rho^0, \bar{\rho}^0, \omega, \bar{\omega}, \rho^+, \bar{\rho}^+\}$ , the spins are parallel and mixing is similarly given by Eq. (2.3). We will work in the good  $SU(2)$  limit with  $m_u = m_d = m$  and with identical spatial extension of wave functions within each P and each V isomultiplet.  $SU(3)$  will be broken in the usual manner taking constituent quark masses with  $m_s > m$  but also, and this is a specific feature of our approach, allowing for different spatial extensions for each P and V isomultiplet. Finally, we will consider that even if gluon annihilation channels may induce  $-m$  mixing, they play a negligible role in VP transitions and thus fully respect the usual OZI-rule.

In our specific case of VP M 1 transitions, these generic statements translate into three characteristic ingredients of the model:

- i) A VP magnetic dipole transition proceeds via quark or antiquark spin- $\frac{1}{2}$  amplitudes proportional to  $q = e_q = 2m_q$ . Apart from the obvious quark charge values, this effective magnetic moment breaks  $SU(3)$  in a well-defined way and distinguishes photon emission from strange or non-strange quarks via  $m_s > m$ .
- ii) The spin- $\frac{1}{2}$  VP conversion amplitude has then to be corrected by the relative overlap between the P and V wave functions. In older papers [10, 11] a common, flavour-independent overlap was introduced. Today, with a wider set of improved data, this new symmetry breaking mechanism can be introduced without enlarging excessively the number of free parameters.
- iii) Indeed, the OZI-rule reduces considerably the possible transitions and their respective VP wave-function overlaps:  $C_s, C_q$  and  $C$  characterize the  $h_s j_s i, h_q j_q i = h_{\bar{q}} j_{\bar{q}} i$  and  $h j_{\bar{q}} i = h j i$  spatial overlaps, respectively. Notice that distinction is made between the  $j_i$  and  $j_{\bar{q}i}$  spatial extension due to the gluon or  $U(1)_A$  anomaly affecting the second state. Independently, we will also need  $C_K$  for the  $hK \bar{K} i$  overlap between strange isodoublets.

It is then a trivial task to write all the VP couplings in terms of an effective  $g = g_{!q} :$

$$\begin{aligned}
 g_{00} &= g_{++} = \frac{1}{3}g ; \quad g_{!} &= g \cos \nu ; \quad g_{-} &= g \sin \nu ; \\
 g_{K^0 \bar{K}^0} &= \frac{1}{3}g z_K - 1 + \frac{m}{m_s} ; \quad g_{K^+ \bar{K}^+} &= \frac{1}{3}g z_K - 2 - \frac{m}{m_s} ; \\
 g_{-} &= g z_q X ; \quad g_{0} &= g z_{\bar{q}} X_{-} ;
 \end{aligned} \tag{3.1}$$

$$\begin{aligned}
g_1 &= \frac{1}{3}g z_q X \cos v + 2\frac{m}{m_s} z_s Y \sin v ; \\
g_1^0 &= \frac{1}{3}g z_q X^0 \cos v + 2\frac{m}{m_s} z_s Y^0 \sin v ; \\
g &= \frac{1}{3}g z_q X \sin v - 2\frac{m}{m_s} z_s Y \cos v ; \\
g^0 &= \frac{1}{3}g z_q X^0 \sin v - 2\frac{m}{m_s} z_s Y^0 \cos v ;
\end{aligned} \tag{3.2}$$

where we have redenoted  $z_q = C_q = C$ ,  $z_s = C_s = C$  and  $z_K = C_K = C$ . The normalization of the couplings is such that  $g_1 = g \cos v = 2(u + d)C \cos v = eC \cos v = m$  and the decay widths are given by

$$(V \rightarrow P) = \frac{1}{3} \frac{g_{VP}^2}{4} \frac{p}{3} = \frac{1}{3} (P \rightarrow V) ; \tag{3.3}$$

where  $p$  is the final photon momentum.

#### 4. Data fitting

We proceed to fit our theoretical expressions for the amplitudes in Eqs. (3.1,3.2) comparing the available experimental information on  $(V \rightarrow P)$  and  $(P \rightarrow V)$  taken exclusively from Ref. [4] with the corresponding decay widths in Eq. (3.3). Looking at these amplitudes, one immediately realizes that the overlapping parameters  $z_{q,s}$  and the mixing parameters  $X_{(0)}$  and  $Y_{(0)}$  cannot be determined independently since they always appear in pairs, namely,  $z_q X_{(0)}$  and  $z_s Y_{(0)}$ . Thus, we start assuming that the overlap of the  $P$  and  $V$  wave functions is maximum, i.e.  $C_q = C_s = C_K = C = 1$  and hence  $z_q = z_s = z_K = 1$ . In addition, we also fix the vector mixing angle  $v$  to its measured value  $\tan v = +0.059$   $0.004$  or  $v = (3.4 \pm 0.2)$  [12] and the ratio of constituent quark masses to  $m = m_s$ ,  $1 = 1.45$ . The fit in this case is very poor,  $\chi^2 = \text{d.o.f.} = 28.3/7$ . The quality of the fit slightly improves when the ratio  $m = m_s$  is left free,  $\chi^2 = \text{d.o.f.} = 17.7/6$  with  $m_s = 1.21 \pm 0.06$ . No improvement is achieved if  $v$  is also left free,  $\chi^2 = \text{d.o.f.} = 16.6/5$  with  $v = (3.3 \pm 0.1)$  and the same for  $m_s = m$  as before.

Clearly, in order to obtain a good fit one has to relax the constraint imposed on the overlapping parameters. In doing so, one gets  $\chi^2 = \text{d.o.f.} = 4.2/4$  with

$$\begin{aligned}
g &= 0.72 \pm 0.01 \text{ GeV}^{-1} ; \quad v = (3.2 \pm 0.1) ; \\
\frac{m_s}{m} &= 1.24 \pm 0.07 ; \quad z_K = 0.89 \pm 0.03 ; \\
z_q X &= 0.65 \pm 0.02 ; \quad z_q X^0 = 0.56 \pm 0.04 ; \\
z_s Y &= 0.52 \pm 0.03 ; \quad z_s Y^0 = 0.58 \pm 0.05 ;
\end{aligned} \tag{4.1}$$

However, as stated before, the mixing parameters  $X_{(0)}$  and  $Y_{(0)}$  cannot be found unambiguously unless a value for the overlapping parameters  $z_q$  and  $z_s$  is provided. This is easily attained if we fix  $X_{(0)}$  and  $Y_{(0)}$  to their expressions under the hypothesis of no

Transition	$g_{V,P}^{\text{exp}}$ (PDG)	$g_{V,P}^{\text{th}}$ (Fit 1)	$g_{V,P}^{\text{th}}$ (Fit 2)
$^0 \pi^0 \pi^0$	0.475	0.024	0.461
$^0 \pi^0 \pi^0$	0.41	0.03	0.41
$\pi^+ \pi^-$	0.140	0.007	0.142
$\pi^+ \pi^-$	0.139	0.015	0.149
$\pi^+ \pi^-$	0.209	0.002	0.209
$\pi^+ \pi^-$	0.22	0.01	0.22

Table 1: Comparison between the experimental values  $g_{V,P}^{\text{exp}}$  for the various  $(V;P)$   $\pi^+ \pi^-$  transitions, with  $P = \pi^0, \pi^+$ , taken from the PDG [4] and the corresponding predictions  $g_{V,P}^{\text{th}}$  from Eqs. (4.2) [Fit 1] and (4.5) [Fit 2], respectively.

gluonium, that is to say  $X_0 = Y_0 = \cos \theta_P$ ,  $X_0 = -Y_0 = \sin \theta_P$ . In this case, the result of the fit is  $\chi^2/\text{d.o.f.} = 4.4/5$  with

$$g = 0.72 \quad 0.01 \text{ GeV}^{-1}; \quad \theta_P = (41.5 \quad 1.2); \quad \theta_V = (3.2 \quad 0.1); \quad (4.2)$$

$$\frac{m_s}{m} = 1.24 \quad 0.07; \quad z_K = 0.89 \quad 0.03; \quad z_q = 0.86 \quad 0.03; \quad z_s = 0.78 \quad 0.05;$$

The fitted values for the two mixing angles  $\theta_P$  and  $\theta_V$  are in good agreement with most results coming from other analyses using complementary information (see, for instance, Ref. [13] and references therein). Our value for the pseudoscalar mixing angle also agrees with the latest measurement from KLOE,  $\theta_P = (41.4 \quad 1.0)$  [1]. The free parameters  $z$ 's are specific of our approach and are not fixed to one as in previous analyses [10, 11]. If we fix the  $z$ 's to unity, the fit gets much worse  $\chi^2/\text{d.o.f.} = 45.9/8$ . This shows that allowing for different overlaps of quark-antiquark wave functions and, in particular, for those coming from the gluon anomaly affecting only the  $\pi^0$  and  $\pi^0$  singlet component, is indeed relevant.

Finally, the symmetry breaking parameter  $m_s/m$  which is essential to adjust the ratio between the two  $K \rightarrow K$  transitions is affected by large uncertainties due to the difficulty in extracting the neutral and charged  $K \rightarrow K$  widths from Primako et al analyses<sup>2</sup>. For these reasons, we have performed a new fit ignoring the two  $K \rightarrow K$  channels. This new fit obviously gives the same results for  $g_{V,P}$  and  $z_q$  whereas  $m_s/m$  and  $z_s$  always appear in the combination  $z_s m_s = m_s$  which is fitted to  $0.63 \quad 0.02$ . Therefore, our results are insensitive to eventual modifications of future and desirable new data on  $K \rightarrow K$  transitions.

In Table 1, we present a comparison between experimental data for the relevant  $V P$  transitions with  $P = \pi^0, \pi^+$  and the corresponding theoretical predictions (in absolute value) calculated from the fitted values in Eq. (4.2). We do not include in that comparison neither  $V \rightarrow \pi^0 \pi^0$  nor  $K \rightarrow K$  modes since they are used to constrain the complementary

<sup>2</sup>The neutral and charged  $K \rightarrow K$  transitions have been measured only by one and two experimental groups, respectively, and seem to need further constraints [4].

parameters  $g$ ,  $v$ ,  $m_s = m$  and  $z_K$ . The agreement is very good and all the predictions coincide with the experimental values within 1%. Notice the small experimental error for the  $g$  coupling as compared to the theoretical one, which, as we will see in Sec. 5, serves to highly constrain the allowed values for the  $-\theta^0$  mixing angle  $\rho$ .

Now that we have provided a value for  $z_q$  and  $z_s$  taken from the fit done under the hypothesis of no gluonium we return to the main issue of this analysis, the phenomenological determination of the gluon content of the  $\pi$  and  $\pi^0$  mesons. Later on, we will comment on the accuracy of this hypothesis. As shown in detail in App. A, due to the orthonormality conditions in Eqs. (A.2, A.3) the mixing pattern of  $\pi$  and  $\pi^0$  is described by means of three independent parameters, which we choose to be  $X$ ,  $X^0$  and  $Y^0$ . Accordingly, the parameters related to the gluonic content,  $Z^2$  and  $Z^2_0$ , and  $Y$  are written in terms of the former ones as

$$\begin{aligned} \mathcal{Y}^{(0)} &= \frac{q}{1 - X^2_{(0)} - Y^2_{(0)}}; \\ Y &= \frac{X^0 X^0 Y^0 + \frac{q}{(1 - X^2_0 - Y^2_0)(1 - X^2 - X^2_0)}}{1 - X^2_0}; \end{aligned} \quad (4.3)$$

In principle, there is a sign ambiguity in the square root of the second term of  $Y$  which in fact is related to the sign ambiguity of the product  $Z^2 Z^2_0$  in Eq. (A.3). Of the two possible choices, the data seems to prefer  $Z^2 Z^2_0 > 0$  thus implying the positive sign in front of that square root. A fit to experimental data is performed imposing the constraints in Eq. (4.3), or equivalently  $X^2_{(0)} + Y^2_{(0)} = 1$  and  $X^0 X^0 + Y^0 Y^0 = 0$ . The results obtained are the following<sup>3</sup>:

$$\begin{aligned} g &= 0.72 \pm 0.01 \text{ GeV}^{-1}; \quad v = (3.2 \pm 0.1); \\ \frac{m_s}{m} &= 1.24 \pm 0.07; \quad z_K = 0.89 \pm 0.03; \\ X &= 0.75 \pm 0.03; \quad X^0 = 0.65 \pm 0.04; \\ Y &= 0.66 \pm 0.04; \quad Y^0 = 0.74 \pm 0.06; \end{aligned} \quad (4.4)$$

with  $\chi^2/\text{d.o.f.} = 4.2/5$ . Note that the value of  $Y$  is obtained from the second expression in Eq. (4.3) and  $z_q, s$  have been fixed to their values in Eq. (4.2). The quality of the fit is similar to the one obtained assuming a vanishing gluonic admixture ( $\chi^2/\text{d.o.f.} = 4.4/5$ ) somewhat anticipating a very small amount of gluonium in the  $\pi$  and  $\pi^0$  wave functions. Using Eq. (4.3) to quantify this statement gives  $Z^2 = 0.00 \pm 0.07$  and  $Z^2_0 = 0.04 \pm 0.10$  (or  $\mathcal{Y}^{(0)} = 0.2 \pm 0.3$ ), where the second value is compatible with zero within 1%. This is one of the main results of our analysis. The current experimental data on  $V P$  transitions seem to indicate a negligible gluonic content for the  $\pi$  and  $\pi^0$  mesons.

In other words, our value for  $Z^2_0$  disagrees with the recent KLOE estimation  $Z^2_0 = 0.14 \pm 0.04$ . As mentioned in Sec. 1, a possible explanation of this discrepancy could be the use in Ref. [1] of old values for the overlapping parameters that the present analysis tries

---

<sup>3</sup>A fit without imposing the constraints in Eq. (4.3) is also feasible. However, the results for the fitted values of the parameters are identical to those of Eq. (4.4).

to update. We perform another  $t$  assuming  $Z = 0$  from the beginning. In this case the mixing parameters can be written in terms of two angles,  $\rho$  and  $\eta_G$ , the latter weighting the gluonic admixture in the  $^0$  (see App. A). Using this angular parametrization one gets  $\rho = (41.4 \pm 1.2)$  and  $j \eta_G j = (11 \pm 13)$  (or  $Z^2_0 = 0.04 \pm 0.09$ ) with  $^2 = \text{d.o.f.} = 4.2/6$ . There is a sign ambiguity in  $\eta_G$  that cannot be decided since this angle enters into  $X^0$  and  $Y^0$  through a cosine. The values we obtain for  $\rho$  and  $\eta_G$  disagree with those reported by KLOE,  $\rho = (39.7 \pm 0.7)$  and  $j \eta_G j = (22 \pm 3)$  [1]. Imposing the constraint  $Z = 0$  also permits a simultaneous  $t$  of the overlapping parameters,  $z_q$  and  $z_s$ , together with the rest of parameters. This new  $t$  allows us to validate the approximation we have done in Eq. (4.4) when we used for a  $t$  assuming the presence of gluonium the values of  $z_{qs}$  obtained from another  $t$  performed under the hypothesis of no gluonium. The results of the new  $t$  are

$$g = 0.72 \pm 0.01 \text{ GeV}^1; \quad \frac{m_s}{m} = 1.24 \pm 0.07; \quad v = (3.2 \pm 0.1);$$

$$\rho = (41.4 \pm 1.3); \quad j \eta_G j = (12 \pm 13); \quad (4.5)$$

$$z_K = 0.89 \pm 0.03; \quad z_q = 0.86 \pm 0.03; \quad z_s = 0.79 \pm 0.05;$$

with  $^2 = \text{d.o.f.} = 4.2/4$ . The fitted values for  $z_q$  and  $z_s$  are compatible with those of Eq. (4.2) thus validating the approximation under discussion and making the whole analysis reliable. This is a second important result of our analysis which in some sense proves or makes more general the one obtained after Eq. (4.4). Accepting the absence of gluonium for the

meson, the gluonic content of the  $^0$  wave function amounts to  $j \eta_G j = (12 \pm 13)$  or  $Z^2_0 = 0.04 \pm 0.09$ . In Table 1, we also include the theoretical predictions for the various transitions involving  $^0$  or  $^1$  calculated from the fitted values in Eq. (4.5). As expected, there is no significant difference between the values obtained allowing for gluonium (Fit 2) or not (Fit 1) in the  $^0$  wave function. For completeness, we predict the value of the ratio

$$R = \frac{(^0 \eta_G ^0)}{(^1 \eta_G ^1)} = \cot^2 \rho \cos^2 \eta_G \cdot 1 \cdot \frac{m_s}{m} \frac{z_q}{z_s} \frac{\tan v}{\sin 2 \rho} \cdot \frac{p_0^2}{p^2} \cdot \frac{p_0^3}{p^3}; \quad (4.6)$$

to be  $(4.7 \pm 0.6) \cdot 10^3$ , in agreement with the experimental value in Ref. [4],  $(4.8 \pm 0.5) \cdot 10^3$ , and the most recent measurement by KLOE [1],  $(4.77 \pm 0.09_{\text{stat}} \pm 0.19_{\text{syst}}) \cdot 10^3$ .

A final exercise we have done is to check whether the very recent measurements (not included in Ref. [4]) on  $^1 \eta_G ^1$  from the SND Coll. [14] and  $^0 \eta_G ^0$  from KLOE [1] modify the results of our analysis. The values of the couplings associated to these new data are displayed in Table 2. As shown, the central values are nearly the same as those from Ref. [4], except for  $^1 \eta_G ^1$ , whereas the errors for  $^1 \eta_G ^1$  are comparable to the world averages and the error for  $^0 \eta_G ^0$  is reduced by a factor of three. Assuming absence of gluonium in the  $^1$  and  $^0$  wave functions the results of the  $t$  are

$$\rho = (42.7 \pm 0.7); \quad z_q = 0.83 \pm 0.03; \quad z_s = 0.79 \pm 0.05; \quad (4.7)$$

with  $^2 = \text{d.o.f.} = 4.0/5$ . Accepting a gluonic admixture in the  $^0$  one obtains

$$\rho = (42.6 \pm 1.1); \quad j \eta_G j = (5 \pm 21); \quad z_q = 0.83 \pm 0.03; \quad z_s = 0.79 \pm 0.05; \quad (4.8)$$

Transition	$g_{V_P}^{\text{exp}}$ (latest)	$g_{V_P}^{\text{th}}$ (Fit 3)	$g_{V_P}^{\text{th}}$ (Fit 4)
$^0 \pi^0$	0.429 0.023	0.436 0.017	0.437 0.028
$^0 \pi^0 \pi^0$	0.41 0.03 (PDG)	0.40 0.02	0.40 0.04
$\pi^+ \pi^-$	0.136 0.007	0.134 0.006	0.134 0.009
$^0 \pi^+ \pi^-$	0.139 0.015 (PDG)	0.146 0.006	0.146 0.013
$\pi^+ \pi^+$	0.214 0.003	0.214 0.017	0.214 0.012
$\pi^- \pi^-$	0.216 0.005	0.216 0.019	0.216 0.018

Table 2: The same as in Table 1 but for  $g_{V_P}^{\text{th}}$  from Eqs. (4.7) | Fit 3 | and (4.8) | Fit 4 |, respectively, compared to the latest  $g_{V_P}^{\text{exp}}$  from Refs. [1, 14].

with  $\chi^2 = \text{d.o.f.} = 4.0/4$ . The values of the remaining parameters are the same as in Eqs. (4.2) and (4.5), respectively. As one can see, the central values for the mixing angle  $\theta_P$  slightly increase while the ones for  $g_G$  (or  $Z^2_0 = 0.01 \dots 0.07$ ) and  $z_q$  decrease. However, in both cases the quality of the fits is as good as it was when only the experimental data provided by Ref. [4] were considered. Moreover, the fitted values of all the parameters are compatible within 1 with those of Eqs. (4.2,4.5). The corresponding theoretical predictions for the  $g_{V_P}$  couplings with  $P = \pi^0$  calculated from the fitted values in Eqs. (4.7) | Fit 3 | and (4.8) | Fit 4 | are also shown in Table 2. Note in this case the small experimental error for  $g_{\pi^0}$  which will constrain even more the allowed values for  $Z^2_0$  (see Sec. 5). In summary, the latest experimental data seem to constrain the nullgluonic content of the  $\pi^0$  and  $\pi^0$  wave functions.

## 5. Comparison with other approaches

Our main results can also be displayed graphically following Refs. [1, 5, 6]. This will serve us to present the bounds obtained using our approach and compare them with other approaches. Very briefly, the analysis of Ref. [5] is based on the SU(3) quark model supplemented by the SU(3) breaking parameter  $m_s = m$  dealing with the difference of the down and strange quark magnetic moments but without taking into account the vector mixing angle  $\theta_V$  or the different vector-pseudoscalar overlapping parameters, both specific features of our approach. The experimental analysis of Ref. [1] is based on the same approach including the latter two features. Finally, the analysis of Ref. [6] utilizes the SU(3) quark model and the vector meson dominance model (VMD). In this framework, the transition amplitudes are expressed in terms of masses and decay constants affected by SU(3) breaking effects.

In Fig. 1, we plot the regions for the  $X$  and  $Y$  parameters which are allowed by the experimental couplings of the  $\pi^0 \pi^0$ ,  $\pi^+ \pi^-$  and  $\pi^+ \pi^+$  transitions (see Table 1). The limits of the bands are given at 68% CL or 1. For the rest of the parameters involved in the determination of the allowed regions we have used the fitted values for  $g_{\pi^0}$ ,  $m_s = m$

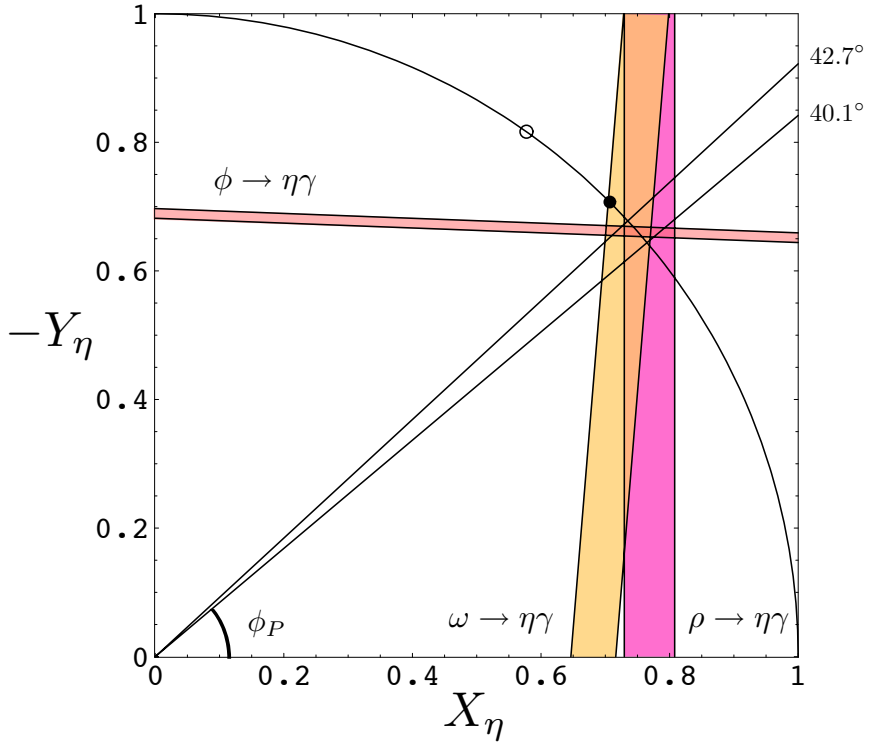


Figure 1: Constraints on non-strange ( $X$ ) and strange ( $Y$ ) quarkonium mixing coefficients in the  $X^2 + Y^2 = 1$  as defined in Eq. (2.1). The circular boundary denotes the constraint  $X^2 + Y^2 = 1$ . The mixing solutions corresponding to the  $\phi$  being a pure octet ( $X = \frac{1}{2}Y = \frac{1}{3}$ ) | open circle| and ( $X = Y = \frac{1}{2}$ ) | closed circle| are shown. The straight lines for the upper and lower bounds of the mixing solution in absence of gluonium,  $\rho = (41.4 \quad 1.3)$ , are also shown. The vertical and inclined bands are the regions for  $X$  and  $Y$  allowed by the experimental couplings of the  $(\phi \rightarrow \eta\gamma, \omega \rightarrow \eta\gamma, \rho \rightarrow \eta\gamma)$  transitions in Table 1.

and  $z_K$  from Eq. (4.4) together with the fitted values for  $z_q$  and  $z_s$  from Eq. (4.2). In addition to the bands, we have also plotted the circular boundary denoting the constraint  $X^2 + Y^2 = 1$  as well as the favoured region for the  $-\theta^0$  mixing angle assuming the absence of gluonium,  $40.1^\circ \leq \rho \leq 42.7^\circ$ , obtained at 1 from the corresponding fitted value in Eq. (4.2). As one can see, there exists a perfect intersection region of the three bands located precisely on the circumference at the region preferred by the mixing angle, thus indicating a vanishing gluonium contribution in the  $\eta$  wave function, i.e.  $\sum_j \rho_j = 0$ . The small size of the intersection region, mainly due to the small experimental error in the  $g$  coupling, and its precise location on the circumference gives strong evidence in favour of the former statement. Notice also the importance of considering the vector mixing angle  $\nu$  different from zero, which translates into a finite slope for the  $(\phi \rightarrow \eta\gamma, \omega \rightarrow \eta\gamma, \rho \rightarrow \eta\gamma)$  bands, in the result obtained. This contrasts with the analysis of Refs. [5, 6] where the vector mixing angle was not taken into account at that time because their effects were covered by the bigger experimental errors of the bands. With the present available experimental

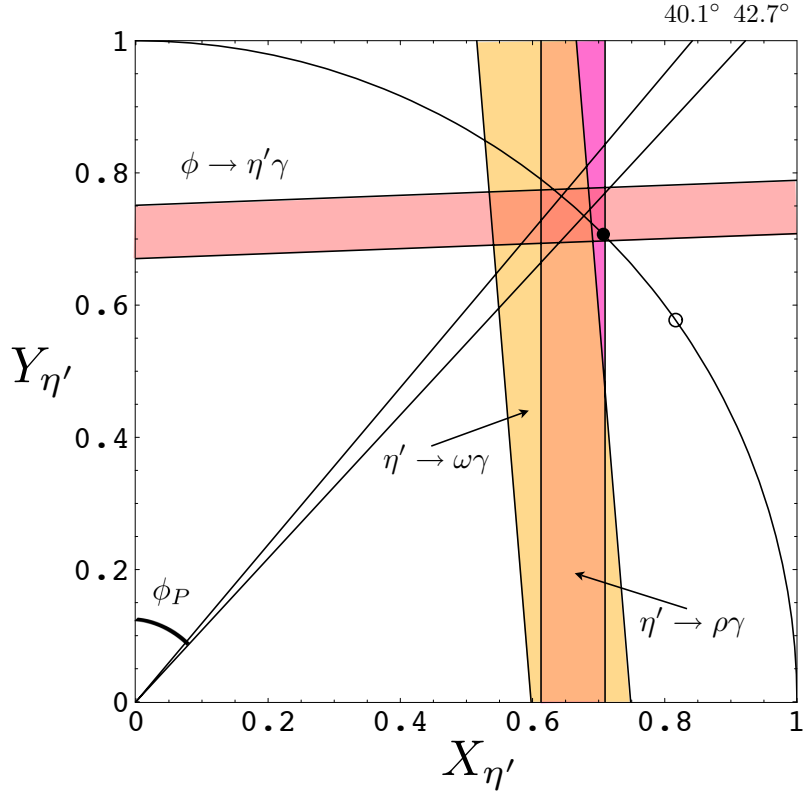


Figure 2: Constraints on non-strange ( $X_{\eta'}$ ) and strange ( $Y_{\eta'}$ ) quarkonium mixing coefficients in the  $\eta'$ . The mixing solutions corresponding to the  $\eta'$  being a pure singlet ( $X_{\eta'} = \frac{1}{2}Y_{\eta'} = \frac{1}{3}$ ) | open circle| and ( $X_{\eta'} = Y_{\eta'} = \frac{1}{2}$ ) | closed circle| are shown. The vertical and inclined bands are the regions for  $X_{\eta'}$  and  $Y_{\eta'}$  allowed by the experimental couplings of the  $\eta' \rightarrow \pi^0 \pi^0$  and  $\eta' \rightarrow \eta^0 \eta^0$  transitions.

data, fixing the value of this angle to zero would have lead to an incompatible solution for the three bands. For completeness, the points corresponding to the  $\eta'$  being a pure octet ( $X_{\eta'} = \frac{1}{2}Y_{\eta'} = \frac{1}{3}$ ) and the "democratic" mixing solution ( $X_{\eta'} = Y_{\eta'} = \frac{1}{2}$ ) are also shown in Fig. 1 as an open and closed circle, respectively. The latter solution, which is now excluded, was still acceptable in the analysis of Ref. [5], where the upper bound  $\beta \gtrsim 0.4$  was obtained from the processes  $\eta' \rightarrow \pi^0 \pi^0$  and  $\eta' \rightarrow \eta^0 \eta^0$ . In Ref. [6], after correcting some inconsistent data, there was no region where all three constraints, coming from the  $\eta' \rightarrow \pi^0 \pi^0$  and  $\eta' \rightarrow \eta^0 \eta^0$  decays, overlap.

The situation is not so constrained for the  $\eta'$  as we proceed to discuss. In Fig. 2, we plot the regions for the  $X_{\eta'}$  and  $Y_{\eta'}$  parameters which are allowed by the experimental couplings of the  $\eta' \rightarrow \pi^0 \pi^0$ ,  $\eta' \rightarrow \eta^0 \eta^0$  and  $\eta' \rightarrow \rho^0 \rho^0$  transitions. Again, we also plot the constraint implied by  $X_{\eta'}^2 + Y_{\eta'}^2 = 1$  and the favoured region for the  $\theta$  mixing angle in absence of gluonium. This time there exists an intersection region of the three bands inside and on the circumference. As most of this region is interior but close to the circular boundary it may well indicate a small but non necessarily zero gluonic content of the

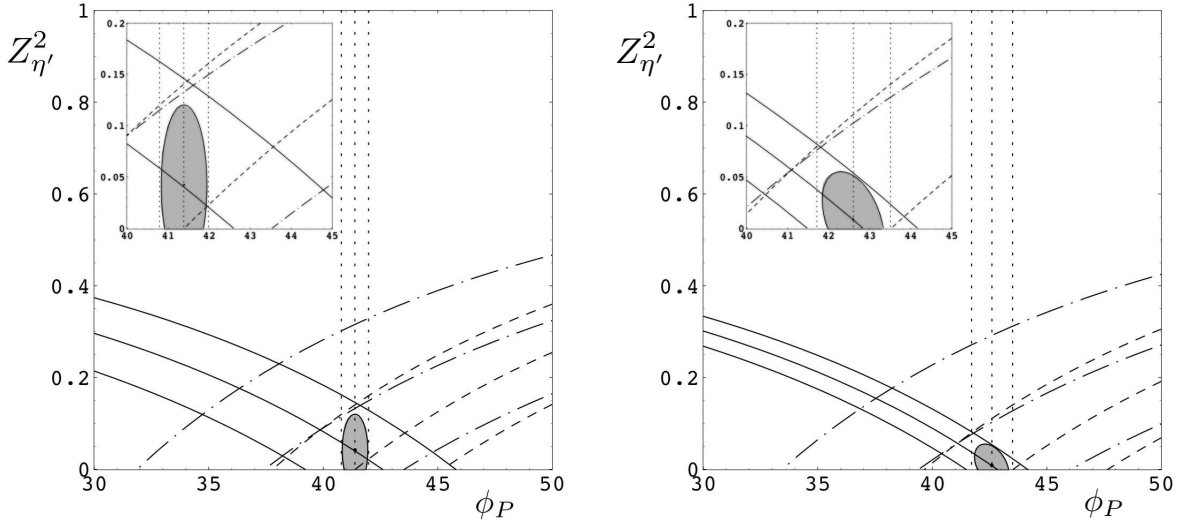


Figure 3: The gray ellipse in the  $(\phi_P; Z_{\eta'}^2)$  plane corresponds to the allowed region at 68% CL of the solution in Eq. (4.5) [left plot] and Eq. (4.8) [right plot], respectively, assuming the presence of gluonium. The different bands are the regions for  $\phi_P$  and  $Z_{\eta'}^2$  allowed by the experimental couplings of the  $^0!^0$  (dashed line),  $^0!^0!$  (dot-dashed line),  $!^0!$  (dotted line), and  $!^0!$  (solid line) transitions in Table 1 [left plot] and Table 2 [right plot], respectively.

$^0$ . Indeed, we have found  $Z_{\eta'}^2 = 0.04 \pm 0.09$  (or  $j_{\eta'} = 0.2 \pm 0.3$ ) or using the angular description  $j_{\eta'} = (12 \pm 13)$ . The size of the error is precisely what prevent us from drawing a definite conclusion concerning the amount of gluonium in the  $^0$  wave function. More refined experimental data, particularly for the  $!^0$  channel, will contribute decisively to clarify this issue (see below). Clearly, the inclusion of this process is of major importance for the determination of the gluonic admixture in the  $^0$ , as observed for the first time in Ref. [5]. In this latter analysis, where  $^0!^0$  and  $^0!^0!$  were used in addition to different values for  $!^0$ , the absence of a significant constraint on  $Y_{\eta'}$  was keenly felt. However, the mixing solution  $X_{\eta'} = Y_{\eta'} = \frac{1}{\sqrt{2}}$  [closed circle in Fig. 2] was still acceptable. It was not the case for the solution identifying the  $^0$  as a pure singlet,  $X_{\eta'} = \frac{1}{\sqrt{2}}Y_{\eta'} = \frac{1}{\sqrt{3}}$ , [open circle in Fig. 2]. In the present analysis, the "democratic" mixing solution is excluded at the 1 level whereas the singlet solution is clearly excluded. In Ref. [6], where  $^0!^0!$  was also included in the analysis, the maximum gluonic admixture in the  $^0$  was obtained to be 26% for  $\phi_P = 11$  (or  $\phi_P' = 44$ ). In our case, for  $Z_{\eta'}^2 = 0.04 \pm 0.09$ , one gets  $R = \frac{Z_{\eta'}^2}{X_{\eta'} + Y_{\eta'} + Z_{\eta'}} = (13 \pm 13)\%$  for  $\phi_P = 41.4$  (or  $\phi_P = 13.4$ ). The same analysis also anticipated that the existence of a gluonic content for the  $^0$  would be excluded for large  $j_{\eta'} j$  (or small  $\phi_P$ ). Finally, the KLOE analysis in Ref. [1] has found a solution allowing for gluonium with  $\phi_P = (39.7 \pm 0.7)$  and  $Z_{\eta'}^2 = 0.14 \pm 0.04$  [or  $j_{\eta'} = (22 \pm 3)$ ], in disagreement, particularly for the  $Z_{\eta'}^2$  value, with our results. A second analysis without the constraint from the  $^0!^0$  decay, which is the less precise, gives  $\phi_P = (39.8 \pm 0.8)$  and  $Z_{\eta'}^2 = 0.13 \pm 0.04$ , thus not modifying their conclusions. To make this difference more graphical, we follow Ref. [1] and plot in Fig. 3 [left plot] the

constraints from  $^0! ( ; !)$  and  $! ( ; ^0)$  in the  $(P; Z^2_0)$  plane together with the 68% CL allowed region for gluonium as obtained from Eq. (4.5). The point corresponding to the preferred solution,  $(P; Z^2_0) = (41.4; 0.04)$ , is also shown. The allowed region is very constrained in the  $P$  axis by the experimental value of the  $g$  coupling, whose vertical band denotes its non dependence on  $Z^2_0$ . The other three bands, all dependent on  $P$  and  $Z^2_0$ , constrain the amount of gluonium down to a value compatible with zero within 1%. As mentioned before, our result differs from the KLOE's one, where  $(P; Z^2_0) = (39.7; 0.14)$  is the preferred solution and the allowed region for gluonium is far from the  $P$  axis (see Fig. 5 in Ref. [1]). The value compatible with zero we have obtained for the gluonic content of the  $^0$  wave function is fully confirmed from a graphical point of view as soon as one includes the latest measurements of the  $! ( ; ^0)$  decays from Refs. [1, 14]. As seen in Fig. 3 [right plot], the allowed region for gluonium decreases due to the smaller experimental error of the  $g_0$  coupling (although the error of  $g_0$  increases a little) and its central point (the preferred solution) is now located at  $(P; Z^2_0) = (42.6; 0.01)$ , even much closer to the  $P$  axis than before.

In all the other approaches discussed so far, the decays  $( ; ^0) !$  were also included in the analyses. As shortly stated in Sec. 1, in our approach we do not take into account these processes since they are well explained using a two mixing angle scenario [7, 8]. Nevertheless, our framework can be extended to describe  $P^0 !$  decays in a similar way to  $V ! P$  and  $P ! V$ . In such case, the needed ratios of decay widths are found to be

$$\begin{aligned} \frac{(^0!)^0}{(^0!)^0} &= \frac{1}{9} \frac{m_0}{m_0}^3 5 z_q X + \frac{P}{2 \frac{m}{m_s}} z_s Y ; \\ \frac{(^0!)^0}{(^0!)^0} &= \frac{1}{9} \frac{m_0}{m_0}^3 5 z_q X_0 + \frac{P}{2 \frac{m}{m_s}} z_s Y_0 ; \end{aligned} \quad (5.1)$$

where, in addition to the parameter  $m = m_s$  related to the different quark spin- $\frac{1}{2}$  effects of the emission of one photon, we have to introduce two new SU(3) breaking parameters,  $z_q = C_q = C$  and  $z_s = C_s = C$ , dealing with the spatial wave functions effects of quark-antiquark annihilation into the other photon. These new parameters are analogous to the overlapping parameters,  $z_q$  and  $z_s$ , of the  $V P$  transitions, and for the same reason, the  $U(1)_A$  anomaly, we also distinguish between the quark-antiquark annihilation effects in  $j_1$  and  $j_{q1}$ . For comparison, in Ref. [5] the former SU(3) breaking effects are not considered, i.e.  $z_q = z_s = 1$  and  $m = m_s = 1$ , while in Ref. [6], where the  $P^0 !$  decays are characterized by means of pseudoscalar decay constants, one identifies  $\frac{f_q}{f} = z_q^{-1}$  and  $\frac{f_s}{f} = \frac{m_s}{m} z_s^{-1}$ . As seen in Eq. (5.1), these ratios are not useful for fixing, within our approach, the mixing parameters of the  $-^0$  system since they also depend on the unknown values of  $z_q$  and  $z_s$ . However, in order to check the consistency of this extended framework, one could use for the mixing parameters and  $m = m_s$  the results obtained from the analysis of  $V ! P$  and  $P ! V$  decays and then fix the values of  $z_{q,s}$  from the two ratios under consideration. In doing so, one gets  $z_q = 0.96 \pm 0.03$  and  $z_s = 0.79 \pm 0.13$  and hence  $f_q = (1.05 \pm 0.03)f$  and  $f_s = (1.57 \pm 0.28)f$ , in agreement with the values  $f_q = (1.10 \pm 0.03)f$  and  $f_s = (1.66 \pm 0.07)f$  found in Ref. [7], thus showing the consistency of the mixing parameters obtained and of the whole approach.

## 6. Summary and conclusions

In this work we have performed a phenomenological analysis of radiative  $V \rightarrow P \gamma$  and  $P \rightarrow V \gamma$  decays with the purpose of determining the gluon content of the  $\pi$  and  $\rho^0$  mesons. The present approach is based on a conventional SU(3) quark model supplemented with two sources of SU(3) breaking, the use of constituent quark masses with  $m_s > m_q$ , thus making the  $V P$  magnetic dipole transitions to distinguish between photon emission from strange or non-strange quarks, and the different spatial extensions for each  $P$  or  $V$  isomultiplet which induce different overlaps between the  $P$  and  $V$  wave functions. The use of these different overlapping parameters [a specific feature of our analysis] is shown to be of primary importance in order to reach a good agreement.

Our conclusions are the following. First, the current experimental data on  $V P$  transitions indicate within our model a negligible gluonic content for the  $\pi$  and  $\rho^0$  mesons,  $Z^2 = 0.00 \pm 0.07$  and  $Z^2_0 = 0.04 \pm 0.10$ . Second, accepting the absence of gluonium for the  $\pi$  meson, the gluonic content of the  $\rho^0$  wave function amounts to  $j_{\pi G} = (12 \pm 13)$  or  $Z^2_0 = 0.04 \pm 0.09$  and the  $\rho^0$  mixing angle is found to be  $\rho = (41.4 \pm 1.3)$ . Third, imposing the absence of gluonium for both mesons one finds  $\rho = (41.5 \pm 1.2)$ , in agreement with the former result. Fourth, the latest experimental data on  $(\pi^+ \pi^- \gamma \gamma)$  and  $\rho^0 \rho^0 \gamma \gamma$  decays confirm the null gluonic content of the  $\pi$  and  $\rho^0$  wave functions. Finally, we would like to stress that more refined experimental data, particularly for the  $\pi^+ \pi^- \gamma \gamma$  channel, will contribute decisively to clarify this issue.

## Acknowledgements

R.E. thanks A. Bramon for a critical reading of the manuscript. This work was supported in part by the Ramon y Cajal program (R.E.), the Ministerio de Educacion y Ciencia under grant FPA 2005-02211, the EU Contract No. MRTN-CT-2006-035482, "FLAVIA net", and the Generalitat de Catalunya under grant 2005-SGR-00994.

## A. Euler angles

In presence of gluonium, the wave functions of the  $\pi$  and  $\rho^0$  mesons and the glueball-like state  $\rho^0$  can be decomposed as

$$\begin{aligned} j_i &= X j_{qi} + Y j_{si} + Z j_{Gi}; \\ j^0_i &= X \bar{o}j_{qi} + Y \bar{o}j_{si} + Z \bar{o}j_{Gi}; \\ j_i &= X j_{qi} + Y j_{si} + Z j_{Gi}; \end{aligned} \quad (A.1)$$

where  $j_{qi} = \frac{1}{2} j_{uu} + d_{di}$ ,  $j_{si} = j_{ss}$  and  $j_{Gi} = j_{G}$  gluonium  $i$ . The  $\pi^+ \pi^- \gamma \gamma$  (1440) state, which we refrain from discussing here, could be identified with the (1405) pseudoscalar resonance (see Ref. [4] for details). The nine coefficients in Eq. (A.1) are constrained by

three normalization conditions

$$X^2 + Y^2 + Z^2 = 1 ;$$

$$X^2_0 + Y^2_0 + Z^2_0 = 1 ; \quad (A.2)$$

$$X^2 + Y^2 + Z^2 = 1 ;$$

and three orthogonality conditions

$$\begin{aligned}
 X_0 X_0 + Y_0 Y_0 + Z_0 Z_0 &= 0; \\
 X_0 X_0 + Y_0 Y_0 + Z_0 Z_0 &= 0; \\
 X_0 X_0 + Y_0 Y_0 + Z_0 Z_0 &= 0;
 \end{aligned} \tag{A.3}$$

Altogether implies that only three independent parameters are required to describe the rotation between the physical states ( $\psi$ ,  $\psi^0$  and  $\psi^1$ ) and the orthonormal mathematical states ( $q_x$ ,  $q_y$  and  $q_z$ ). The rotation matrix can be written in terms of three mixing angles,  $\theta_x$ ,  $\theta_y$  and  $\theta_z$ , which would correspond to the three Euler angles for a rotation in real, three-dimensional space. Explicitly,

$$0 = \begin{matrix} & C & 0C & G & & S & 0C & G & & S & G \\ S & 0S & 0G & C & 0S & 0G & S & G & C & 0C & 0G & + & S & 0S & 0G & S & G & S & 0G & C & G \\ S & 0S & 0G & + & C & 0C & 0G & S & G & C & 0S & 0G & S & 0C & 0G & S & G & C & 0G & C & G \end{matrix} ; (\mathbb{A} \cdot \mathbb{A})$$

with  $(c; s) = (\cos; \sin)$ . In the limit in which  $g_G = \eta_G = 0$ , the gluonium decouples and the former matrix reduces to the usual rotation matrix describing  ${}^0m$  mixing,

$$0 = \begin{matrix} & C & 0 & S & 0 & & q \\ 0 & & S & 0 & C & 0 & & s \end{matrix} ; \quad (A.5)$$

where  $\theta_p$  is the mixing angle in the quark-avour basis related to its octet-singlet basis analog through  $\theta_p = \theta_{p-} \arctan \frac{p_+}{2}$ ,  $\theta_{p-} = 54.7^\circ$ . An interesting situation occurs when the gluonium content of the meson is assumed to vanish, i.e.  $\theta_G = 0$ . In this particular case,

$$X = \cos P ; \quad Y = \sin P ; \quad Z = 0 ; \quad (A.6)$$

$$X_0 = \sin P \cos \theta_G ; \quad Y_0 = \cos P \cos \theta_G ; \quad Z_0 = \sin \theta_G ;$$

## References

- [1] F. Ambrosino et al. [LOE Collaboration], arXiv:hep-ex/0612029.
- [2] A. Alasio et al. [LOE Collaboration], Phys. Lett. B 541 (2002) 45 [arXiv:hep-ex/0206010].
- [3] A. Bramon, R. Escribano and M. D. Scadron, Phys. Lett. B 503 (2001) 271 [arXiv:hep-ph/0012049].
- [4] W. M. Yao et al. [Particle Data Group], J. Phys. G 33 (2006) 1.
- [5] J. L. Rosner, Phys. Rev. D 27 (1983) 1101.
- [6] E. Kou, Phys. Rev. D 63 (2001) 054027 [arXiv:hep-ph/9908214].

- [7] R. Escribano and J.M. Frere, JHEP 0506 (2005) 029 [[arXiv:hep-ph/0501072](https://arxiv.org/abs/hep-ph/0501072)].
- [8] T. Feldmann, Int. J. Mod. Phys. A 15 (2000) 159 [[arXiv:hep-ph/9907491](https://arxiv.org/abs/hep-ph/9907491)].
- [9] G. Li, Q. Zhao and C. H. Chang, [arXiv:hep-ph/0701020](https://arxiv.org/abs/hep-ph/0701020).
- [10] N. Isgur, Phys. Rev. Lett. 36 (1976) 1262.
- [11] P. J. O'Donnell, Rev. Mod. Phys. 53 (1981) 673.
- [12] S. I. Dolinsky et al., Phys. Rept. 202 (1991) 99.
- [13] A. Bramon, R. Escribano and M. D. Scadron, Eur. Phys. J. C 7 (1999) 271 [[arXiv:hep-ph/9711229](https://arxiv.org/abs/hep-ph/9711229)].
- [14] M. N. Achasov et al., Phys. Rev. D 74 (2006) 014016 [[arXiv:hep-ex/0605109](https://arxiv.org/abs/hep-ex/0605109)].